Chemical Tuning of the Microphase Separation in Diblock Copolymers from Controlled Radical Polymerization

D. Bendejacq,† V. Ponsinet,* and M. Joanicot†

Complex Fluids Laboratory, UMR 166 CNRS/Rhodia, Cranbury, New Jersey 08512-7500

A. Vacher and M. Airiau

Centre de Recherche d'Aubervilliers, 52 Rue de la Haie Coq, 93308 Aubervilliers, France

Received May 12, 2003

ABSTRACT: We investigate whether block copolymers of controlled effective segregation strength can be designed via a novel controlled radical polymerization technique that allows statistical polymerization of different monomers in either one of the constituting blocks: We examine the morphologies and segregation regimes of two families of poly(styrene-*stat*-(acrylic acid))-*b*-poly(acrylic acid) diblocks of different block ratios (i.e., one asymmetric and one symmetric), comprising a statistical first block of variable ratio of styrene vs acrylic acid and a second PAA block. Thanks to small-angle X-ray scattering and transmission electron microscopy, we observe that as the composition of the statistical first block is varied, such asymmetric and symmetric diblocks form strongly to weakly microphase-separated structures, respectively, presenting spherical and well-ordered lamellar symmetries, or homogeneous (disordered) phases. We thus demonstrate that the segregation strength can be quantitatively controlled by the composition of the statistical first block, regardless of the diblock symmetry.

Introduction

Diblock copolymers self-assemble in the melt state when the segregation strength between the building blocks is large enough.[1−3] This segregation strength is usually measured by the product χN of the Flory−Huggins segment−segment interaction parameter χ between the two blocks and the total polymerization degree N of the chains. On the other hand, the morphology of the microphase-separated structure (when present) is governed principally by the volume ratio of the blocks, usually referred to as the composition of the diblock.

The microphase separation results from the simultaneous antagonistic requirements of (i) maximizing the blocks conformational entropy and the entropy of mixing of the chains and (ii) minimizing the enthalpic cost that arises from the unfavorable contacts between the different chemical species present in the building blocks. Therefore, low values of χ or N entropically favor a homogeneous (disordered) state for the diblock chains. When χ or N increase enough, the enthalpic cost required to keep in contact the two species in the disordered state dominates the entropic gain, and a microphase separation occurs. This event is called the order−disorder transition (ODT), and it is predicted by the self-consistent-field theory (SCFT)[3] to occur at a critical value $(\chi N)_{ODT}$ of about 10 for symmetric diblocks, while for increasingly asymmetric diblocks, $(\chi N)_{ODT}$ is predicted to increase. Regardless of the diblock symmetry, different segregation regimes have been described for $\chi N > (\chi N)_{ODT}$: (i) the "weak segregation" regime,[2,4] closest to the ODT, characterized by a finite width of the domains interface and blocks of nearly Gaussian conformation, and (ii) the "strong segregation" regime,[3,5] far from the ODT, characterized by sharp boundaries between domains and fairly extensive stretching of the blocks. For a given diblock molecular weight, the more incompatible the species, the more stretched the chains and therefore the larger the spacing of the structure. In the case of strongly segregated monodisperse diblock copolymers, Semenov[6] derived a relation between the structure spacing d, the chain molecular weight N, and the Flory parameter χ: $d_0 \propto N^{2/3}\chi^{1/6}$. It was recently proposed[7] that this relation is also valid in the weak segregation regime. While the dependence with N was easily verified experimentally thanks to a simple screening of different degrees of polymerization,[8] the dependence with χ has been checked in very few cases[7] due to the very limited variations obtained through temperature modulation, a method usually chosen to change the value of χ. The variations of structure spacing and object size accessible through the tuning of χ are thus quite limited, which makes almost impossible the independent choice of molecular weight and microstructure sizes, once the chemical natures of the blocks are imposed. A posteriori chemical alterations of either of the two blocks were successfully used to selectively modify the segregation strength without having to change the degree of polymerization or the temperature, but require extra postpolymerization reactions.[7,9] A priori tuning of the chemical natures of the monomers involved in each block seems to be a convenient route to achieve a substantial control over the chemical incompatibility between blocks, but was until now restricted to the families of monomers polymerizable through the classical techniques.

The development of controlled radical polymerization (CRP) techniques over the past decade[10−13] has greatly expanded the possibilities of architectures and the variety of monomers that can be incorporated into block copolymers. Although the technique can yield, in some cases, polydispersity indices as low as those obtained through anionic polymerization, polymers produced by CRP are in general substantially polydisperse. However,

† Present address: Centre de Recherche d'Aubervilliers, 52 Rue de la Haie Coq, 93308 Aubervilliers, France.

* Author for correspondence: e-mail virginie.ponsinet@us.rhodia.com.

10.1021/ma0302661 CCC: $25.00
Published on Web 08/22/2003

Table 1. Compositions and Molecular Weights of the Diblocks and Characteristic Sizes of the Structures

sample	f_{B1}[a]	φ_{AA}[b]	M_n[c]	N[d]	Φ_{AA}[e]	d[f] (Å)	R[g] (Å)	phase[h]	s_O[i] (Å^2)
C1	0.089	0.00	16 000	154	0	N/A	N/A	correlated	N/A
A1	0.164	0.00	17 050	164	0	245	88	Sph	121
A2	0.167	0.140	15 800	152	0.084	241	80	Sph	130
A3	0.169	0.242	16 300	157	0.141	229	74	Sph	148
A4	0.149	0.517	18 500	178	0.329	~267	N/A	correlated	N/A
A5	0.165	0.737	16 400	158	0.596	N/A	N/A	disorder	N/A
S1	0.565	0.00	17 990	173	0	337	95	L	170
S2	0.574	0.185	17 800	171	0.101	284	81	L	207
S3	0.549	0.420	17 900	172	0.265	209	57	L	283
S4	0.559	0.761	17 980	173	0.610	~185	N/A	correlated	N/A

[a] The first block volume fraction f_{B1} for all P(S-*stat*-AA)-*b*-PAA diblocks was computated from the ^{1}H NMR data using for the density of the first block the same value $d_{PS} = 1.05$ g/cm^3 of a pure PS homopolymer and for the density of the second block $d_{PA} = 1.47$ g/cm^3 (see ref 14). [b] φ_{AA} is approximated as $\varphi_{AA} = \varphi_{EA}$ (see text), where φ_{EA} is measured by ^{1}H NMR experiments on the aliquot first blocks (see Table 2). [c] Total number-average molecular weight M_n of the diblock in g/mol, computed from the molecular weight of the first P(S-*stat*-AA) block as computed from SEC measurement and from the ^{1}H NMR composition of the diblock (both results not shown here). [d] N is the equivalent total polymerization degree as computed from the total molecular weight M_w using a reference monomer segment, i.e., styrene. [d] Equivalent volume fraction of acrylic acid segments in the first block Φ_{AA} as computed from the molar composition φ_{AA} using a reference monomer segment volume, i.e., that of styrene. [e] The characteristic interdomain distances are extracted from the positions of the first correlation peak in the SAXS spectra. [f] R is the radius of the spheres of the first block for the A-family, extracted from the SAXS spectra using eq 1 (see text), whereas it is the half-thicknesses of the first block lamellae for the S-family, computed from f_{B1} and d. [g] "Sph" and "L" designate phases of spherical objects with no long-range order and lamellar phases, respectively. "Correlated" indicate the presence of a single broad correlation peak in the SAXS spectrum, interpreted as the onset of microphase separation. "Disorder" corresponds to a featureless SAXS pattern and a homogeneous sample. [h] The area per chain at the interface between the domains is computed using f_{B1}, d, R, and the total polymerization degree.

the extensive polydispersity accompanying CRP techniques was proven to have no adverse effect on the phase behavior and microdomain order in poly(styrene)-*b*-poly(acrylic acid) diblocks,[14] for which spherical (Sph) phases with no long-range order, and cylindrical (C) and lamellar (L) phases with long-range order, were identified. A major advantage of the CPR techniques is the possibility to produce block copolymers in which each block can fairly easily be made a statistical copolymer of two or more different chemical functions: this feature may offer a new way of controlling the segregation strength in block copolymers via a chemical tuning of the blocks incompatibility and could then allow an almost independent choice of copolymer molecular weights, chemical species, and segregation regimes.

Using a novel CRP technique (MADIX), developed by Rhodia,[15−17] we investigate the segregation strength and morphology of solvent-cast films of poly(styrene-*co*-(acrylic acid))-*b*-poly(acrylic acid) diblock copolymers (P(S-*stat*-AA)-*b*-PAA), of variable first block composition and with different diblock symmetries. To the best of our knowledge, this work is the first systematic investigation of segregation as a function of the chemical composition of one of the blocks and varying the block ratio, for any CRP-derived diblock family.

Experimental Section

Diblock Synthesis and Sample Preparation. Poly(styrene-*stat*-ethyl acrylate)-*b*-poly(ethyl acrylate) diblock copolymers, P(S-*stat*-EA)-*b*-PEA, were synthesized via the MADIX approach[15−17] in aqueous emulsion. The concentrations of polymer latexes were close to 30% (w/w) at the end of the synthesis. The first block was synthesized by simultaneous continuous additions of precise amounts of styrene and ethyl acrylate monomers so as to obtain controlled molar fractions φ_{EA} of ethyl acrylate and $(1 - \varphi_{EA})$ of styrene in the block. The second PEA block was then polymerized in the presence of 2−5 wt % methacrylic acid comonomer for polymerization stability reasons only. Two diblock families of different symmetries were investigated: an asymmetric family denoted A (melt volume fraction of the first block $f_{B1} \approx 0.16$, in all cases) and a symmetric one denoted S ($f_{B1} \approx 0.56$ in all cases), both with a total polymerization degree always close to 220. An additional very asymmetric poly(styrene)-*b*-poly(ethyl acrylate) ($\varphi_{EA} = 0$) denoted C1 was synthesized ($f_{B1} \approx 0.089$; total polymerization degree 218). In all cases, aliquot precursor first blocks (P(S-*stat*-EA), φ_{EA}) were sampled from the reactor prior to polymerization of the second PEA block. In particular, we sampled a homogeneous series of P(S-*stat*-EA) aliquot first blocks of constant molecular weight (approximately 8 kg/mol, i.e., 100 monomer units) with an increasing molar fraction φ_{EA} of ethyl acrylate, listed in Table 2.

Table 2. Compositions of Aliquot First Blocks of Constant Molecular Weight (8 kg/mol)

sample	φ_{EA}[a] expected	φ_{EA}[b] measured
M1	0.000	0.000 ± 0.011
M2	0.052	0.048 ± 0.011
M3	0.104	0.092 ± 0.011
M4	0.155	0.150 ± 0.011
M5	0.206	0.185 ± 0.011

[a] Ethyl acrylate molar fraction added in the reactor during polymerization. [b] Ethyl acrylate molar fraction measured by ^{1}H NMR experiments on the aliquot first blocks. The systematic experimental error is ±0.011, as estimated from the integration of the 3.6−4.3 ppm region in the ethyl acrylate-free M1 sample.

The molecular weight and polydispersity of the aliquot first blocks and those of the diblocks were measured by gel permeation chromatography (GPC), using a series of Phenogel columns, tetrahydrofuran (THF) as eluent (1 mL/min), and a differential refractive index detector. The system was calibrated with narrow-distribution PS standards. The PS and PEA hydrodynamic volumes differ at fixed molecular weight, as do their refractive index increments in THF. The apparent number-average molecular weight M_n and polydispersity index PI are therefore only approximations of the actual values. Polydispersity indices are all found between 2 and 2.5.

The ethyl acrylate units were then hydrolyzed to sodium acrylate units in a sealed glass reactor with NaOH (2 mol per mole of acrylate functional group coming from the diblock) for 24 h at 90−95 °C, with a diblock concentration of about 4 wt %. The solution was then precipitated into aqueous HCl at pH 1, redispersed in a water/THF mixture, and extensively dialyzed against aqueous HCl (pH 2.5) to purify the polymer and completely convert the acrylic acid units to their acidic form. The polymer was finally isolated by freeze-drying.

^{1}H NMR spectroscopy (Varian Unity Inova 400 MHz) measurements were performed on the first blocks and on the diblocks before and after hydrolysis, in solution in deuterated pyridine, to quantify the hydrolysis efficiency, the statistical nature of the first block, and the first block and diblock

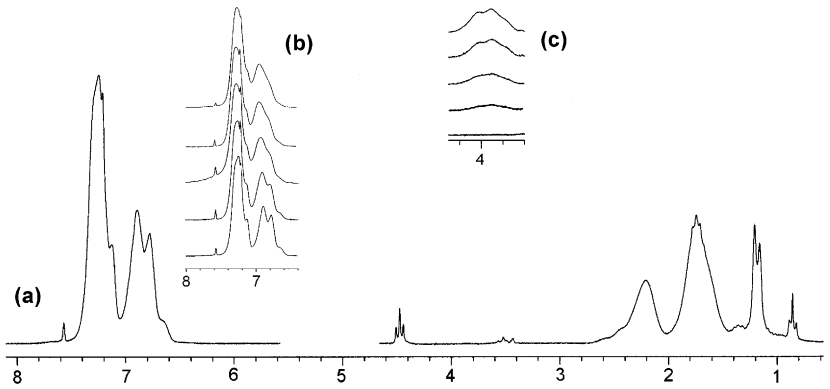

Figure 1. ^{1}H NMR spectra for unhydrolyzed poly(styrene-*stat*-ethyl acrylate) aliquot first blocks of constant molecular weight 8 kg/mol, with an increasing fraction of ethyl acrylate: (a) homopolymer of styrene, showing a featureless (3.6−4.3 ppm) region; (b) close-up on region 6.4−8.0 ppm, showing increasing broadening of styrene-associated peaks and shifting to higher values of the chemical shift δ, as the fraction of ethyl acrylate is increased; and (c) close-up on region 3.6−4.3 ppm, showing broad ethyl acrylate-associated peaks of increasing intensity as the fraction of ethyl acrylate is increased.

compositions. Molecular characteristics of the diblocks, all of constant total molecular weight of approximately 16 kg/mol, are presented in Table 1.

Films were slowly cast (3−4 days) from 15 to 20 wt % solutions in THF (a good solvent for both PS and PAA) in poly(tetrafluoroethylene) molds, then placed overnight under vacuum at room temperature, and finally heated for an hour at 60 °C to remove traces of THF. The final films were 0.2−0.4 mm thick.

Morphological Characterization. Small-angle X-ray scattering (SAXS) and transmission electron microscopy (TEM) were used to identify the lattice types and spacings of the diblocks, all at room temperature using the solvent-cast films described above. Although the films were not temperature-annealed prior to morphological characterization, we assume that they are close enough to the equilibrium morphologies.[14]

All SAXS profiles were acquired in transmission, using the small-angle chamber of a multiangle X-ray diffractometer system (MAXS) at the Laboratory for Research on the Structure of Matter of the University of Pennsylvania, Philadelphia. A rotating anode X-ray generator (Bruker-Nonius) delivers a high-brightness radiation in a 0.2 × 2 mm^2 spot. Doubly focusing mirror−monochromator optics (Molecular Metrology, Inc.) provide a 1:1 focusing at the detector. A multiwire detector (Bruker Hi-Star) allows acquisition of a two-dimensional scattering pattern, which is subsequently integrated. The final spectrum presents the scattered intensity $I(q)$ in arbitrary units, as a function of the wave vector $q = (4\pi/\lambda) \sin \theta$, where λ is the wavelength of the Cu Kα radiation and θ is half the scattering angle. In Figures 3 and 4, the SAXS intensities for specimens exhibiting a lamellar phase are multiplied through by q^2, as a first-order correction for the impact of the form factor $P(q)$ of individual lamellae, while no correction is made to those for specimens exhibiting a spherical phase. Thus, the peak positions in $q^2I(q)$ or $I(q)$ correspond more closely to the peaks in the lattice's structure factor $S(q)$, from which the interdomain spacing d can be extracted.

For transmission electron microscopy (TEM), films were embedded in epoxy and cured at 50 °C. Slices of 100 nm thickness were obtained at room temperature with an Ultracut E ultramicrotome (Reichert-Jung) and were exposed for 10 min to vapors of an aqueous solution of RuO_2 and $NaIO_4$, which preferably stains the PS domains, before examination on a JEOL 1200 EX TEM at 120 kV.

Results and Discussion

Diblock Composition and Molecular Structure. ^{1}H NMR experiments were performed on the homogeneous series of P(S-*stat*-EA) aliquot first blocks with an increasing molar fraction φ_{EA} of ethyl acrylate, listed in Table 2, to determine whether the copolymerization of styrene and ethyl acrylate in the first block of P(S-*stat*-EA)-*b*-PEA diblock copolymers is truly statistical and whether the expected compositions of these P(S-*stat*-EA) blocks are attained. Figure 1a presents the entire ^{1}H NMR spectrum of a pure polystyrene block, while parts b and c show the evolution as φ_{EA} is increased, of two specific regions of this spectrum.

More precisely, Figure 1b shows the broadening of the 6.5−7.4 ppm resonance peaks associated with the five hydrogen atoms on the benzene ring of the styrene function, increasingly shifted toward larger values of the chemical shift δ as φ_{EA} is increased. The broadening and the shift in position are both consistent with differences in the local environment of the benzene ring caused by the presence of statistically copolymerized ethyl acrylate functions. Figure 1a also shows that the 3.6−4.3 ppm region in the spectrum of a pure PS is featureless, while Figure 1c shows a double peak of increasing height as φ_{EA} is increased, which we associate with the ethyl acrylate functions. This peak is much broader (3.6−4.3 ppm, cf. Figure 1c) and shifted compared to the usual position of the narrow multiple peaks found at 4.0−4.6 ppm for homopolymerized ethyl acrylate functions (cf. Figure 2a). Although φ_{EA} is increased, the latter characteristic peak remains absent in the spectrum of a P(S-*stat*-EA) block, which demonstrates the absence of homopolymerized ethyl acrylate sequences in the P(S-*stat*-EA) first blocks. Note that as φ_{EA} goes beyond 0.5, the shift between the peak of homopolymerized EA functions of the second block and the peak of statistically polymerized EA of the first block diminishes and the two peaks eventually merge.

We conclude that the copolymers constituting the first blocks do not have a significant blocky microstructure and can therefore be considered as really statistical. Similar results were obtained on the aliquot first blocks precursor to the asymmetric family.

Integration of the 3.6−4.3 ppm region (EA) and the 6.6−7.8 ppm region (styrene) in each case gives access to the actual composition φ_{EA} of the aliquot first blocks, which is found in very good agreement with the amount added in the polymerization reactor (see Table 2). The same type of analysis on diblocks gives access to the diblock composition, detailed in Table 1.

^{1}H NMR experiments were also performed on the diblocks before and after hydrolysis to determine the efficiency of the hydrolysis reaction. Figure 2 presents, as an example, the ^{1}H NMR spectra for (a) the unhydrolyzed poly(styrene)-*b*-poly(ethyl acrylate) precursor

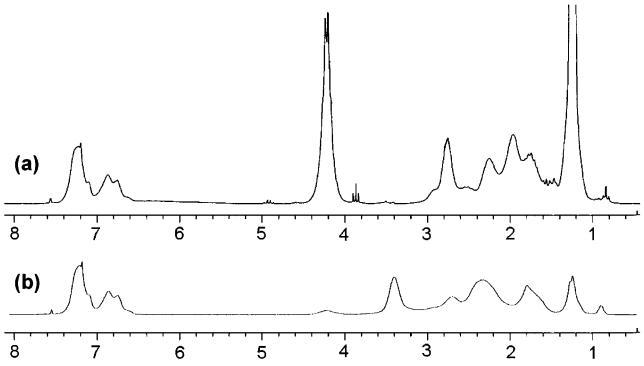

Figure 2. ^{1}H NMR spectra for (a) unhydrolyzed poly(styrene)-*b*-poly(ethyl acrylate) precursor to diblock (A1) and (b) hydrolyzed poly(styrene)-*b*-poly(acrylic acid) diblock (A1).

to diblock (A1) and (b) the hydrolyzed poly(styrene)-*b*-poly(acrylic acid) diblock (A1). As mentionned above, homopolymerized ethyl acrylate functions give multiple, fairly narrow peaks between 4.0 and 4.6 ppm (cf. Figure 2a). After hydrolysis, we measure that only a small fraction of this signal remains, while a narrow 3.2−3.6 ppm peak appears, characteristic of homopolymerized acrylic acid functions. Integration of the residual 4.0−4.6 ppm ethyl acrylate signal provides a way to quantify the global hydrolysis yield of the diblocks. The hydrolysis yields of ethyl acrylate functions of the first and second blocks (respectively statistically copolymerized with styrene and homopolymerized) are bound to be different because of a difference of environment during the reaction of hydrolysis in water. In the cases of PS-*b*-PEA samples A1 and S1 ($\varphi_{EA} = 0$), both with first blocks of pure PS, integration of the residual 4.0−4.6 ppm ethyl acrylate peak provides a reliable way to determine the hydrolysis efficiency of the second block alone: we found that the hydrolysis yield of the second block is equal to 99 ± 1%. In the cases of the asymmetric and symmetric P(S-*stat*-EA)-*b*-PEA diblocks with a fraction φ_{EA} of EA in the first block close to 0.5, the integration of the ethyl acrylate peaks led to a global hydrolysis efficiency of 96.5% and 98.7% for samples A4 ($\varphi_{EA} = 0.52$) and S3 ($\varphi_{EA} = 0.42$), respectively. These values, which cumulate the hydrolysis efficiencies of EA functions present in both blocks, prove that a majority (64 ±15% for A4 and 98 ±2% for S3) of the EA functions of the first block are hydrolyzed. Therefore, in the following, the molar fraction φ_{AA} of acrylic acid in the first block after hydrolysis is simply approximated to $\varphi_{AA} = \varphi_{EA}$ for all samples.

Segregation and Structures of the Diblocks. The SAXS patterns obtained on polymer films from the symmetric (asymmetric) diblock family are presented in Figure 3 (Figure 4). For both families, three distinct types of patterns are obtained, depending on the value of φ_{AA}. For the smallest values of φ_{AA}, single or multiple intense sharp structure factor peaks are observed, whereas for the highest value of φ_{AA}, featureless scattering spectra are obtained. These two cases obviously correspond to the segregated and disordered (homogeneous) states, respectively, which are classically observed with segregative block copolymers. The third case corresponds to intermediate values of φ_{AA}, for which we observe a single broad correlation peak, characteristic of the so-called concentration fluctuations effect, in the onset of phase separation in segregative diblock copolymers.[4]

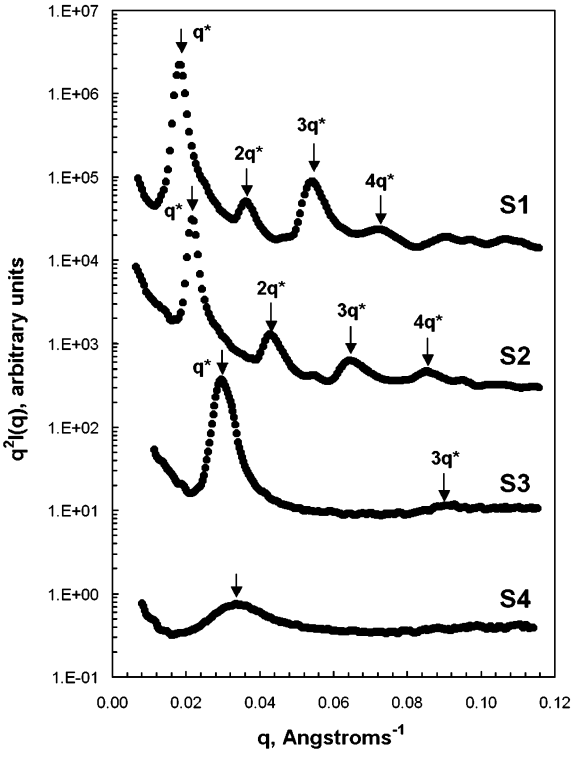

Figure 3. SAXS data (logarithmic intensity scale) for the diblocks from the symmetric family S1 to S4, from top to bottom. Spectra of samples S1 to S3 are consistent with well-ordered lamellar microdomains. The intensities of the even-order reflections are much weaker than the ones of the odd-order reflections, which indicates a near-volume symmetry in these lamellar systems. The broad peak in spectrum of sample S4 is consistent with the concentration fluctuations characteristic of a sample near the order−disorder transition.

More precisely, in the case of the symmetric diblocks, the upper three curves S1, S2, and S3 (cf. Figure 3) exhibit sharp multiple peaks at q-to-q^* ratios of 1:2:3, where q^* is the position of the primary peak, consistent with well-ordered lamellar structures (L-phase). Such long-range order was previously shown to occur in similar systems despite the significant molecular weight polydispersities that characterize the polymers obtained through this CRP technique.[14] For all well-ordered lamellar diblocks, the intensities of the even-order reflections are weaker than those of the odd-order reflections, indicating that the alternating domains are of approximately same thickness. Indeed, such cancellation of a structure factor peak is a classical signature of the near-volume symmetry of a lamellar system and is due to the proximity of a form factor node to the position of a structure factor peak.[18] As the molar fraction φ_{AA} increases, both the long-range lamellar order and the volume symmetry appear to be preserved, but the peaks diminish in height, get broader, and are displaced toward larger values of wave vector q: the larger the value of φ_{AA}, the smaller the lamellar spacing $d = 2\pi/q^*$ calculated from the position of the first-order peak q^* (values listed in Table 1). Eventually, for the lower curve (S4), the pattern does not present peaks anymore, and only a broad correlation peak is visible. The SAXS results on samples S1 and S3 were confirmed by transmission electron microscopy on thin sections of films. The corresponding TEM images are shown in parts a and b of Figure 5, respectively. In both cases, the images consist of long well-ordered stripes, which we identify with an L phase. In agreement with the

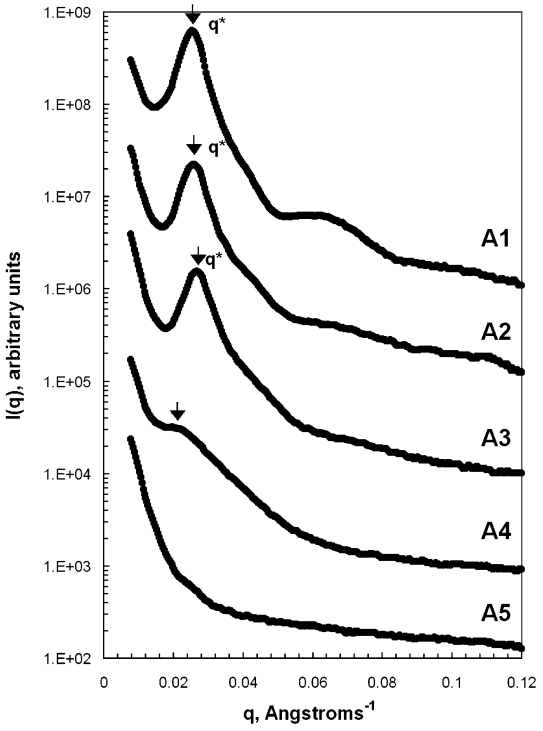

Figure 4. SAXS data (logarithmic intensity scale) for the diblocks from the asymmetric familly A1 to A5, from top to bottom. Spectra of samples A1 to A3 are consistent with spherical microdomains with no long-range order. The spectrum of sample A5 shows the absence of a microphase separation and is identified as disordered (homogeneous). In between, the broad peak in the spectrum of sample A4 is consistent with the concentration fluctuations characteristic of a sample near the order−disorder transition.

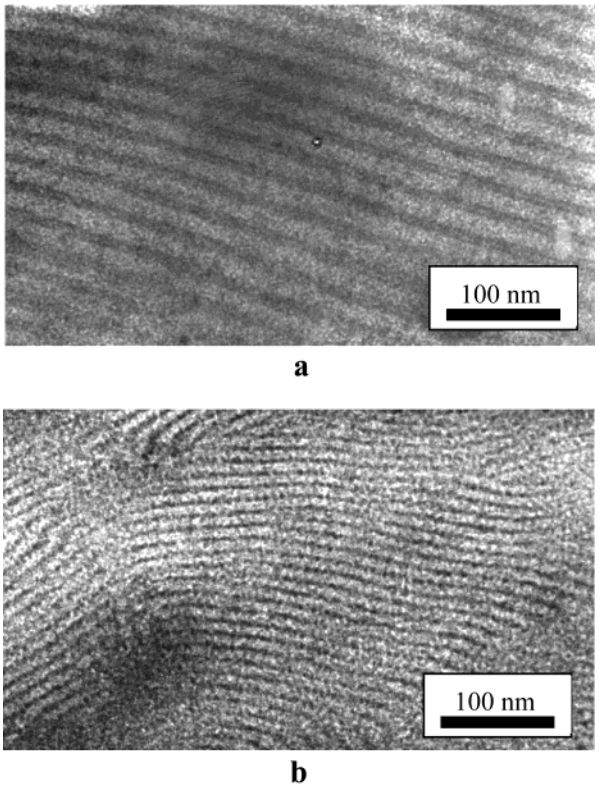

Figure 5. TEM images obtained on stained sections of symmetric diblocks S1 (a) and S3 (b), showing large (1−2 μm) domains of long stripes, which are identified as lamellar domains. The images show the near-volume symmetry of both systems, in agreement with the SAXS spectra (cf. Figure 3).

SAXS results, we measure that the lamellar periodicity of sample S3 (cf. Figure 5b) is significantly smaller than that of sample S1 (cf. Figure 5a) in which the first block is pure PS. TEM images also confirm that both lamellar phases are nearly symmetric in volume.

In contrast to the well-ordered L phases observed with the symmetric diblocks, the samples from the asymmetric family exhibit no lattice order, whatever the value of φ_{AA}, in agreement with previous results.[14] On the upper curve of Figure 4 (sample A1), the scattering pattern resembles that obtained for a liquidlike packing of spheres:[19,20] a primary peak with an intermediate-q shoulder, followed at higher q by one or more well-defined oscillations, characteristic of the contribution to the scattering of the form factor of isolated quasi-monodisperse spheres. As φ_{AA} increases from 0 (sample A1) to 0.242 (sample A3) (cf. Figure 4), the form factor oscillations become less pronounced and shift toward larger q values, indicating a decrease in the object size. The form factor minima and maxima observed experimentally are compared to the theoretical form factor scattering $P_S(q)$ of isolated monodisperse dense spheres of radius R:[21]

$$P_S(q) \propto \left[\frac{\sin qR - qR\cos qR}{q^3R^3}\right]^2 \qquad (1)$$

and equivalent sphere radii are extracted (cf. Table 1). At the same time, the unique correlation peak slightly shifts to larger q values as φ_{AA} increases. Characteristic center-to-center distances $d = 2\pi/q^*$ are extracted from the positions of the correlations peaks q^* and are listed in Table 1. Both form factor oscillations and correlation peak eventually disappear for a large enough value of φ_{AA}, and the SAXS spectrum of sample A5 is essentially featureless.

As a conclusion, the systems go from microphase-separated to homogeneous via a weak segregation regime: we demonstrate that, regardless of the diblock symmetry, an order−disorder transition (ODT) can be chemically induced at constant degree of polymerization N and temperature T.

Characteristic Sizes. As measured from the SAXS and confirmed by TEM, the interdomain spacings d and the size of the domains formed by the first blocks decrease when φ_{AA} is increased, for both diblock symmetries (cf. Table 1). The difference in molecular volume between acrylic acid segments and styrene segments could play a role in this decrease, but it cannot be the dominant effect as it would then also alter the volume symmetry of the lamellar phases. Indeed, both SAXS and TEM experiments show that the lamellar spacing is reduced by a factor of almost 2 when going from S1 to S3, while the phases remains nearly symmetric in volume. The decrease in characteristic sizes rather corresponds to a decreasing segregation strength between the two blocks: Indeed, as φ_{AA} is increased, the chemical incompatibility between the blocks decreases, leading to an increase of the surface of contact and a decrease of the stretching of the blocks. Finally, this stretching decrease directly results in a decrease of the domain sizes. From the decrease of the lamellar spacing when going from S1 to S3, we compute that the area per chain s_O increases from 170 to 283 Å^2. On the other hand, the SAXS experiments also show that the radius of the spherical core in the case of the asymmetric family can be varied by at least 16% when going from A1 to

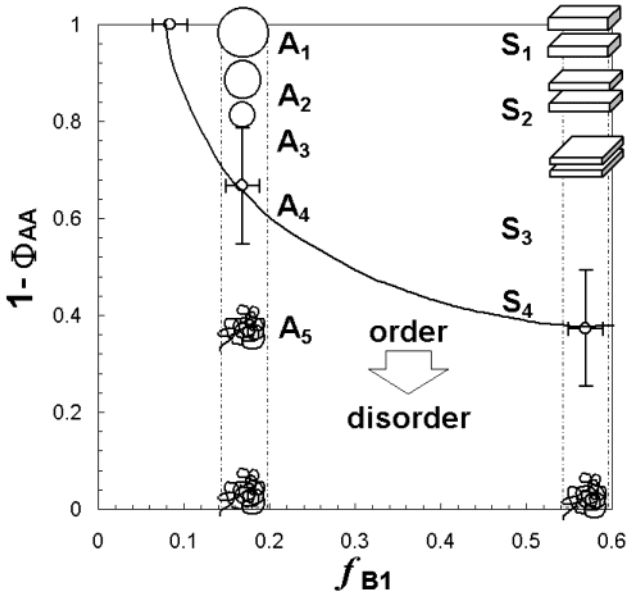

Figure 6. Phase diagram of poly(styrene-*stat*-(acrylic acid))-*b*-poly(acrylic acid), represented as a function of the volume fraction f_{B1} of the first block on the *x*-axis, and the equivalent molar fraction of styrene in the first block ($1 - \Phi_{AA}$) on the *y*-axis. The full line is a guide for the eye representing the position of the order−disorder transition.

A3, which results in an increase of the area per chain s_O from 121 to 148 Å^2 and accordingly to a corresponding decrease of over 40% for the aggregation number $g = 4\pi R_S^2/s_O$ of these spherical domains. Therefore, the chemical tuning of the first statistical block offers a significant control over the characteristic sizes of the microstructures and consequently over their aggregation numbers and surface density.

Phase Diagram. To reach a semiquantitative analysis of the observed order−disorder transition, we interpret as being the closest to the transition the samples exhibiting the unique broad correlation peak characteristic of a concentration fluctuations effect, and we assume that their first block molar composition roughly corresponds to the transition composition. As a result, the ODT's are identified at different critical values of the molar composition, depending on diblock symmetry. More precisely, working within the framework of a Flory-type analysis, we calculate the equivalent total polymerization degree *N* and the equivalent molar fraction Φ_{AA} based on a reference monomer volume, namely that of styrene (cf. Table 1). Indeed, the basic theory of block copolymer segregation is based solely on the use of such reference quantities, for it assumes equality in the densities, monomer volumes, and Khun lengths in the species involved, except when specified otherwise due, in particular, to conformational asymmetry.[22] Such considerations go beyond the scope of the present article, and the diblocks are here treated as ideal systems. The identified ODT's values are $(\Phi_{AA})_{ODT} = 0.33 \pm 0.1$ for diblocks from the asymmetric ($f_{B1} = 0.16$) family and $(\Phi_{AA})_{ODT} = 0.63 \pm 0.1$ for those from the symmetric ($f_{B1} = 0.56$) family. In addition, sample C1 ($\Phi_{AA} = 0$, $f_{B1} = 0.085$) was found to present the same SAXS signature and was also identified as being close to the ODT (SAXS spectrum not shown). These results are summarized in the phase diagram of poly(styrene-*stat*-(acrylic acid))-*b*-poly(acrylic acid) diblock copolymers, presented in Figure 6, in which the ODT line is located according to the critical values indicated above.

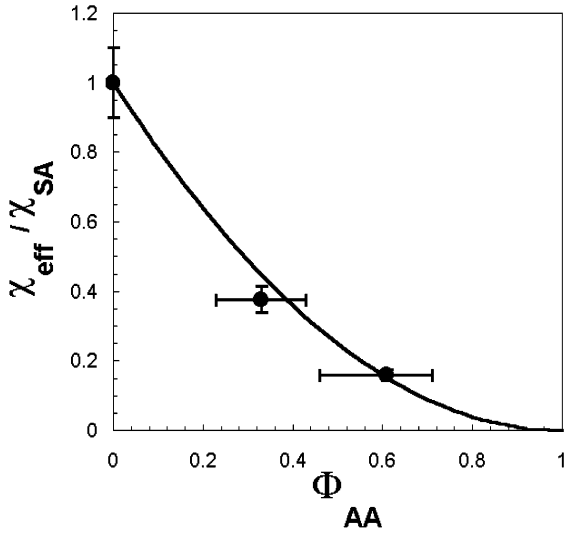

Figure 7. Experimental data obtained at the ODT (circles) and mean-field calculation (line) of the relative effective interaction parameter: χ_{eff}/χ_{SA} as a function of the equivalent molar fraction Φ_{AA} of acrylic acid monomers in the first block.

This particular phase diagram, at constant temperature and constant total degree of polymerization *N*, is plotted as a function of diblock symmetry on the *x*-axis (through the volume fraction f_{B1} of the P(S-*stat*-AA) block) and the molar fraction ($1 - \Phi_{AA}$) of styrene in the first block on the *y*-axis. As is clear from the resemblance of this phase diagram with the phase diagram $\chi N - f_{B1}$ classically drawn for segregative diblock copolymers, there is a quantitative analogy between the composition ($1 - \Phi_{AA}$) of the first block and the effective segregation strength $\chi_{eff}N$ between the two blocks. In particular at the ODT, a unique function links $(\chi_{eff}N)_{ODT}$ to $(1 - \Phi_{AA})_{ODT}$. In the next section, we describe the evolution of the effective segregation strength, and we develop a simple model based on Flory-type arguments to account for it.

Effective Interaction Parameter. In a self-consistent-field approach, Matsen and Bates[3] predict that the ODT should occur at $(\chi N)_{ODT} = 62$, 27, and 10.5 for diblocks of compositions $f_{B1} = 0.089$, 0.16, and 0.56, respectively. For a given diblock symmetry f_{B1}, and knowing the value of *N* in our diblocks, we use these predicted values of $(\chi N)_{ODT}$ to extract the value χ_{eff} of the effective interaction parameter at the location of the ODT: $\chi_{eff} = (\chi N)_{ODT}/N$. By definition, in the case of sample C1 ($\Phi_{AA} = 0$, $f_{B1} = 0.089$, $N = 154$), the value χ_{eff} ($\Phi_{AA} = 0$) computed is simply equal to the interaction parameter χ_{SA} between pure styrene and acrylic acid blocks: χ_{eff} ($\Phi_{AA} = 0$) $\equiv \chi_{SA} = 0.40 \pm 0.03$. For samples A4 ($\Phi_{AA} = 0.33$, $N = 178$) and S4 ($\Phi_{AA} = 0.61$, $N = 172$), we find χ_{eff} ($\Phi_{AA} = 0.33$)/$\chi_{SA} = 0.152/0.40 \approx 0.38$ and χ_{eff} ($\Phi_{AA} = 0.61$)/χ_{SA} ($\Phi_{AA} = 0$) $= 0.064/0.40 \approx 0.16$, respectively. These results are represented in Figure 7, in which we plot χ_{eff}/χ_{SA} as a function of Φ_{AA} at the ODT.

We observe that χ_{eff} monotonicaly decreases as Φ_{AA} is increased. This apparent decrease of the segregation strength between the two blocks can be regarded as solely resulting from a decrease of this effective interaction parameter χ_{eff}, defined as the interaction parameter between equivalent chemical functions. Using a simple Flory-like approach, we count the probabilities of contact between the different monomers and find $k_BT\chi_{eff} = \epsilon_{SA}(1 - \varphi_{AA}) + \epsilon_{AA}\varphi_{AA} - {}^1/_2[\epsilon_{AA} + \epsilon_{AA}\varphi_{AA}^2 + \epsilon_{SS}(1 - \varphi_{AA})^2 + 2\epsilon_{SA}\varphi_{AA}(1 - \varphi_{AA})]$, where ϵ_{SS}, ϵ_{AA}, and ϵ_{SA} are the

energies required to form (styrene−styrene), (acrylic acid−acrylic acid), and (styrene−acrylic acid) contacts, respectively. Such mean-field considerations, in agreement with previous treatments of homopolymer/statistical copolymer binary blends,[23,24] lead to the prediction that the effective parameter should vary as $\chi_{eff}/\chi_{SA} = (1 - \Phi_{AA})^2$, where by definition $k_B T\chi_{SA} = \epsilon_{SA} - {}^1/_2[\epsilon_{AA} + \epsilon_{SS}]$. Figure 7 shows that the values of χ_{eff} extracted from our experimental data are in good quantitative agreement with this prediction.

Conclusion

We have demonstrated that controlled radical polymerization can produce diblocks of tunable effective segregation strength by statistically copolymerizing two different monomers in one of the blocks. The morphologies and segregation regimes of poly(styrene-*stat*-acrylic acid)-*b*-poly(acrylic acid) diblock copolymers of variable block ratios show that the segregation strength is quantitatively controlled by statistically tuning the composition of one of the blocks. Microphase separation, which is useful for many applications, can thus be prevented or induced by statistical copolymerization of an antagonistic monomer in either of the two blocks. This could be done for a variety of block chemistries and independently of the molecular weight of the diblocks and allows a better control of the characteristic sizes of the microstructures.

Acknowledgment. We are very thankful to Mathias Destarac and Gilda Lizzaraga, Rhodia, for support in the synthesis work, to Heiko Mauermann, Rhodia, for help on the NMR study, and to Karen Winey, University of Pennsylvania, for help on the SAXS experiments.

References and Notes

(1) Hamley, I. W. *The Physics of Block Copolymers*; Oxford University Press: New York, 1998.
(2) Bates, F. S.; Fredrickson, G. H. *Annu. Rev. Phys. Chem.* **1990**, *41*, 525.
(3) Matsen, M. W.; Bates, F. S. *Macromolecules* **1996**, *29*, 1091.
(4) Leibler, L. *Macromolecules* **1980**, *13*, 1602.
(5) Helfand, E.; Wasserman, Z. R. In *Developments in Block and Graft Copolymers-1*; Goodman, I., Ed.: Applied Science Publishers: New York, 1982; p 99.
(6) Semenov, A. N. *Sov. Phys. JETP* **1985**, *61*, 733.
(7) Ren, Y.; Lodge, T. P.; Hillmyer, M. A. *Macromolecules* **2002**, *35*, 3889.
(8) Hashimoto, T. *Macromolecules* **1982**, *15*, 1548.
(9) Lee, K. M.; Han, C. D. *Macromolecules* **2002**, *35*, 760.
(10) Matyjaszewski, K., Ed.; *Controlled Radical Polymerization;* ACS Symposium Series 685; American Chemical Society: Washington, DC, 1998.
(11) Matyjaszewski, K.; Xia, J. *Chem. Rev.* **2001**, *101*, 2921.
(12) Hawker, C. J.; Bosman, A. W.; Harth, E. *Chem. Rev.* **2001**, *101*, 3661.
(13) Kamigaito, M.; Ando, T.; Sawamoto, M. *Chem. Rev.* **2001**, *101*, 3689.
(14) Bendejacq, D.; Ponsinet, V.; Joanicot, M.; Loo, Y.-L.; Register, R. A. *Macromolecules* **2002**, *35*, 6645.
(15) Corpart, P.; Charmot, D.; Zard, S. Z.; Biadatti, T.; Michelet, D. US Patent #6,153,705, Nov 28, 2000, to Rhodia Chimie.
(16) Destarac, M.; Charmot, D.; Franck, X.; Zard, S. Z. *Macromol. Rapid Commun.* **2000**, *21*, 1035.
(17) Charmot, D.; Corpart, P.; Adam, H.; Zard, S. Z.; Biadatti, T.; Bouhadir, G. *Macromol. Symp.* **2000**, *150*, 23.
(18) Chu, J. H.; Rangarajan, P.; Adams, J. L.; Register, R. A. *Polymer* **1995**, *36*, 1569.
(19) Adams, J. L.; Quiram, D. J.; Graessley, W. W.; Register, R. A.; Marchand, G. R. *Macromolecules* **1996**, *29*, 2929.
(20) Kinning, D. J.; Thomas, E. L. *Macromolecules* **1984**, *17*, 1712.
(21) Guinier, A.; Fournet, G. *Small-Angle Scattering of X-Rays*; Wiley: New York, 1955.
(22) Lai, C.; Russel, W. B.; Register, R. A.; Marchand, G. R.; Adamson, D. H. *Macromolecules* **2000**, *33*, 3461.
(23) Kambour, R. P.; Bendler, J. T.; Bopp, R. C. *Macromolecules* **1983**, *16*, 753.
(24) ten Brinke, G.; Karasz, F. E.; MacKnight, W. J. *Macromolecules* **1983**, *16*, 1827.

MA0302661